NANOSYSTEMS:
PHYSICS, CHEMISTRY, MATHEMATICS

Dahiya S., et al. *Nanosystems: Phys. Chem. Math.*, 2024, **15** (5), 632–642.
http://nanojournal.ifmo.ru
DOI 10.17586/2220-8054-2024-15-5-632-642

Original article

Tuning the nonlinear optical properties of a 1D excitonic GaAs quantum dot system under a semi-parabolic potential with a detailed comparison with the experimental results: interplay of hydrostatic pressure and temperature

Suman Dahiya[1], Siddhartha Lahon[2,a], Rinku Sharma[1,b]

[1]Department of Applied Physics, Delhi Technological University, Delhi 110042, India
[2]Physics Department, KMC, University of Delhi, Delhi 110007, India

[a]sid.lahon@gmail.com, [b]rinkusharma@dtu.ac.in

Corresponding author: Siddhartha Lahon, sid.lahon@gmail.com

ABSTRACT The present study is dedicated to study the effect of Temperature and Hydrostatic Pressure on the absorption coefficient and refractive index of one-dimensional semi-parabolic excitonic GaAs QD's by applying the compact density matrix formalism. Calculations are performed to obtain the excitonic state wave functions and energies in the strong confinement regime using the effective mass approximation. A significant dependence of nonlinear optical refractive index and absorption coefficient on hydrostatic pressure and temperature can be observed for excitonic and without excitonic case. Our investigations show that the peaks blue/red shifts are substantial when the excitonic interactions are taken into account. The opposite effects caused by temperature and pressure have substantial practical importance as they extend an alternative approach to tune and control the optical frequencies resulting from the transitions. The comparative analysis of the analytical optical properties of excitonic system facilitates the experimental identification of these transitions which are often close. We have attempted a comparison of the absorption coefficient obtained in the present work with experimental data at $T \cong 10$ and 100 K and found that the theoretical prediction is in agreement for $T \cong 10$ K and it is in slight deviation from the experimental data for higher temperatures. The whole of these conclusions may have broad implications in future designing of Optoelectronic devices.

KEYWORDS nanostructures, quantum dot, exciton, nonlinear effects, hydrostatic pressure, temperature

ACKNOWLEDGEMENTS We acknowledge sincere gratitude to Delhi Technological University to appreciate their help and enhance our services and facilities.

FOR CITATION Dahiya S., Lahon S., Sharma R. Tuning the nonlinear optical properties of a 1D excitonic GaAs quantum dot system under a semi-parabolic potential with a detailed comparison with the experimental results: interplay of hydrostatic pressure and temperature. *Nanosystems: Phys. Chem. Math.*, 2024, **15** (5), 632–642.

1. Introduction

The semiconductor nanomaterials such as quantum dots (QD), quantum wires and quantum wells have many applications in the generation of optoelectronic devices such as lasers, infrared and THz photodetectors, solar cells, biological imaging devices, photovoltaics, LEDs, etc., owing to their enchanting physical properties due to the quantum confinement effects in all spatial directions [1–5]. Out of all these nanostructures, quantum dots of various shapes, sizes and strong confinement of electron and holes have been given special attention as they possess interesting physics in terms of the unique electronic and optical properties. Quasi-zero-dimensional quantum dots can be considered as nano crystalline structures that can provide limitless utility in the implementation of many semiconductors' optoelectronic devices such as quantum dot solar cells, spintronics and ultrafast quantum computers. Accordingly, unprecedented attention has been given to the semiconductor nanomaterials in the last few decades [6–13].

The parabolic and semi parabolic confinement potential can allow various resonances, due to the constant spacing of the discrete energy levels which accounts for the enormous enhancement of the nonlinear optical susceptibilities, optical transitions within the valence and conduction band, and absorption properties [14–17]. Furthermore, the parabolic and semi parabolic potential confinement is more relevant when the zero-dimensional quantum dots are fabricated by using an etching process, ion implantation or electrostatic gates. We have found considerable investigations on the nonlinear optical and electronic properties such as Refractive Index (RI), Absorption Coefficient (AC) and Rectification Coefficient (RC) with photon energy and external factors such as temperature, hydrostatic pressure and dot size [18–20]. For photons having energies equal to that of inter-subband transition energies, host material finds a significant change in dielectric constant, thereby inducing changes in the nonlinear excitonic optical properties [21–24].

Numerous investigations and interesting studies are done on the nonlinear optical properties of nanostructures especially Quantum dots under the influence of external factors such as electric field, magnetic field etc. [21–30]. Many

authors studied the effect of excitons in one dimensional semi parabolic quantum dots [31–34]. Duque et al. studied the effect of external factors such as electric field, magnetic field, hydrostatic pressure, laser field and temperature on nonlinear properties in excitonic system [35–38]. Bejan et al. demonstrated the effect of electric field on the optical properties of a semi parabolic quantum dot in an excitonic system [39]. Kumar et al. further investigated the effect of hydrostatic pressure, temperature and spin on the optical and electronic properties of nanostructures [40,41]. To summarize, the interesting results of the ramifications of external factors such as hydrostatic pressure, temperature, electric field and magnetic field on the nanostructures bring out plethora of novel and exciting physical properties.

The main objective of the present work is to investigate the effect of external factors such as temperature and hydrostatic pressure on the RI and AC of excitonic system in 1D semi parabolic quantum dot. An excitonic system is a bound electron-hole pair with more closely matched effective masses that is formed by the electrostatic interaction between the electron and hole. Theoretically, this system can be related to the hydrogenic system and it possess discrete energies. A 1D QD is principally a nanostructure which can be assumed as a small portion of a 1D QW which is bordered by a two-wall potential. The charge carriers are free to move along the wire in 1-D QW, whereas they are restricted to move along the spatial length in 1D QD [27, 42–45]. The core study undertaken in this research paper focuses on a one-dimensional semi parabolic quantum dot, which is strongly confined in the x and y direction and electrons and holes are confined by a semi parabolic potential along the z direction. We know that the hydrostatic pressure and temperature can alter the nonlinear properties such as the refractive index and absorption coefficient for excitonic effects (EE) as well as without excitonic effect (WEE). In order to keep the study concise and in line with the experimentally available results, we have restricted our studies to the two extreme limits of a temperature range 10 – 100 K where it is observed that the sharpest absorption peaks or transmittance dips are observed at low temperatures in the mentioned range or even lower than that. Furthermore, it is observed that as temperature increases above 100K, the value of the thermal excitation energy of the charge carriers, namely $kT/2$, attains significant values.

In our recent work, we have reported the effect of temperature and hydrostatic pressure on the optical rectification associated with the excitonic system in a semi-parabolic quantum dot [46]. It is highlighted that most available literature reports are primarily based on the nonlinear optical properties due to impurities or due to different shape of quantum structures. To our sincere understanding, there are no studies available where the hydrostatic pressure and temperature effects on the nonlinear optical properties of excitonic system in one dimensional semi parabolic quantum dots have been studied and explained. The present paper is structured as follows: In the next section, theoretical analytical framework is presented to calculate the eigen energies, eigen functions and optical properties for the excitonic system. In the Results and Discussion section, we have presented our numerical results and discussion. In the last section of conclusion, we have summarized our results.

2. Theory and model

A theoretical model of the system taken is presented in Fig. 1. Here, the gate voltage in the model is used to control Rashba spin-orbit interaction (SOI) where the effects of SOI are studied. In our case, we have kept the gate voltage to be Zero. The x-direction is kept to be very small i.e., about 2nm so that the charge carriers behave as a 2D charge carrier gas. The y-length of the wire is in μm-range, so the charge carrier exhibit e^{-ky} wave function. The z-directions breadth is determined by the potential strength and in our case, the effective z-length turns out to be 5 nm. Now, moving towards the mathematical calculations related to the system.

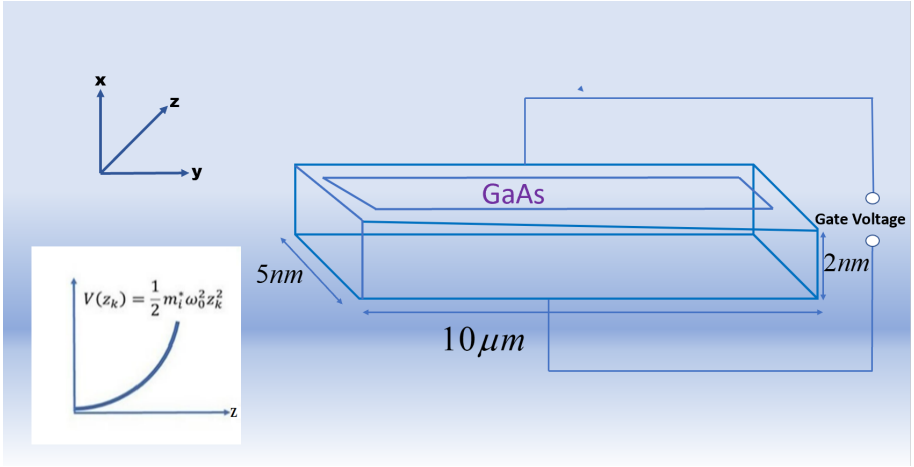

FIG. 1. Schematic diagram of GaAs Quantum Dot

Hamiltonian for a 1D excitonic QD having semi-parabolic confining potential within the framework of effective mass approximation can be written as [25, 27, 31, 42]:

$$H_e = \frac{p_h^2}{2m_h^*(P,T)} + \frac{p_e^2}{2m_e^*(P,T)} + V(z_e) + V(z_h) - \frac{e^2}{\varepsilon\,|z_e - z_h|}, \tag{1}$$

where $z_e, z_h > 0$.

Here m_h^* and m_e^* represents the effective mass of hole and electron, respectively, ε represents the background dielectric constant and the last term represents the electrostatic Coulomb interaction term between the electron and the hole. The semi-parabolic confinement potential $V(z_k)$ is written as:

$$V(z_k) = \begin{cases} \frac{1}{2} m_i^* \omega_0^2 z_k^2, & z_k \geq 0; \\ \infty, & z_k \leq 0 \quad (k = e, h). \end{cases} \tag{2}$$

The temperature and hydrostatic pressure dependent effective mass of the electron for GaAs is given as [38, 40, 41]:

$$m_e^*(P,T) = m_o \left[1 + \frac{7510}{E_g(P,T) + 341} + \frac{15020}{E_g(P,T)}\right]^{-1}, \tag{3a}$$

$$m_h^*(P,T) = \left(0.09 - 0.20 \cdot 10^{-3} P - 3.55 \cdot 10^{-5} T\right) m_0, \tag{3b}$$

with

$$E_g(P,T) = \left[1519 - \frac{0.5405 T^2}{T + 204} + 10.7P\right]. \tag{4}$$

Here temperature and hydrostatic pressure dependent energy gap GaAs, E_g is in meV, P is in "kbar" and T is in "Kelvin". The pressure dependent oscillator frequency is expressed as

$$\omega(P) = \omega_0 / \left[1 - 2P(1.16 \cdot 10^{-3} - 7.4 \cdot 10^{-4})\right]. \tag{5}$$

The Hamiltonian is segmented into two terms taking the relative motion and the center of mass into consideration and is given by:

$$H_{e1} = H_{r1} + H_{c1}, \tag{6}$$

$$H_{r1} = \frac{p^2}{2\mu} + \frac{1}{2}\mu\omega_0^2 z_{r1}^2 - \frac{e^2}{\varepsilon(P,T)\,|z_{r1}|}, \tag{7}$$

$$H_{c1} = \frac{P^2}{2M_{T1}} + \frac{1}{2} M_{T1} \omega_0^2 Z_{T1}^2. \tag{8}$$

For $T < 200$, the dielectric constant of GaAs is [38–40]:

$$\varepsilon(P,T) = 12.74 e^{(9.4 \cdot 10^{-5})(T - 75.6) + 1.73 \cdot 10^{-3} P}. \tag{9}$$

The coordinate of the centre of mass is written as:

$$Z_{T1} = \frac{m_h^*(P,T) z_h + m_e^*(P,T) z_e}{M_{T1}}. \tag{10}$$

Here, total mass is $M_{T1}(P,T) = m_h^*(P,T) + m_e^*(P,T)$; the relative coordinate is $z_{r1} = z_e - z_h$, the momentum operator is $p_{Z_{T1}} = \frac{\hbar}{i} \nabla_{Z_{T1}}$, and the reduced mass is

$$\mu_{r1} = m_h^*(P,T) m_e^*(P,T) / M_{T1}(P,T). \tag{11}$$

The excitonic wave function and energy levels are written as

$$\psi_{f1}(z_h, z_e) = \phi(z_{r1}) \varphi(Z_{T1}), \tag{12}$$

$$E_{T1} = E_{z_{r1}} + E_{Z_{T1}}. \tag{13}$$

The term signifying the center of mass part is considered as the problem for 1D semi-parabolic oscillator where the Hamiltonian is H_{c1} and eigenfunction and eigenenergies are [42]:

$$\varphi_{k1}(Z_{T1}) = N_{k1} \exp\left(-\frac{1}{2}\alpha^2 Z_{T1}^2\right) H_{2k1+1}(\alpha Z_{T1}), \tag{14}$$

$$E_{k1} = \left(2k1 + \frac{3}{2}\right)\hbar\omega_0, \quad k1 = (0, 1, 2.....), \tag{15}$$

where H_{2k1+1} is the Hermite polynomial

$$N_{k1} = \left[\frac{1}{\alpha}\sqrt{\pi} 2^{2k1} (2k1 + 1)!\right]^{-1/2}, \tag{16}$$

$$\alpha = \sqrt{M_{T1}\omega(P)/\hbar_k}. \tag{17}$$

We analytically obtained the eigenvalues and wave function of the relative motion part in the strong and weak confinement regime. For the strong regime, H_{r1} reduces to:

$$H_{r1s} = \frac{p^2}{2\mu} + \frac{1}{2}\mu\omega_0^2 z_{r1}^2. \tag{18}$$

Neglecting the coulomb term as per the strong confinement regime, $\varphi(z_{r1})$ is determined as:

$$\phi(z_{r1}) = N_n \exp\left[-\frac{1}{2}\beta^2 z_{r1}^2\right] H_{2n+1}(\beta z_{r1}), \tag{19}$$

$$E_{y1} = \left(2n + \frac{3}{2}\right)\hbar\omega_0, \quad (y1 = 0, 1, 2, ...), \tag{20}$$

$$N_n = \left[\frac{1}{\beta}\sqrt{\pi}2^{2n1}(2n+1)!\right]^{-1/2}, \tag{21}$$

$$\beta = \sqrt{\mu\omega(P)/\hbar}. \tag{22}$$

Our quantum dot interacts with the electromagnetic field $E(t)$ having a frequency ω, such that [47–49]:

$$E(t) = Ee^{i\omega t} + E^* e^{-i\omega t}. \tag{23}$$

Upon such interactions, the time evolution equation for the matrix elements of one-electron density operator, ρ, is given by

$$\frac{\partial\rho}{\partial t} = \frac{1}{i\hbar}\left[H_0 - qxE(t)\rho\right] - \Gamma(\rho - \rho^{(0)}), \tag{24}$$

where H_0 represents the Hamiltonian of this system in the absence of the electromagnetic field $E(t)$, and electronic charge is given by q, unperturbed density matrix operator is ρ^0, and Γ is the phenomenological operator responsible for the damping due to the electron-phonon interaction, collisions among electrons, etc. It is assumed that Γ is a diagonal matrix and its elements are equal to the inverse of relaxation time τ_0.

For solving Eq. (19), standard iterative method is being used and hence ρ has been expanded as $\rho(t) = \sum_n \rho^{(n)}(t)$. Now, using this expansion in Eq. (19), the density matrix elements can be obtained as shown below:

$$\frac{\partial\rho_{ij}^{(n+1)}}{\partial t} = \left[\frac{1}{i\hbar}[H_0, \rho^{(n+1)}]_{ij} - \Gamma_{ij}\rho_{ij}^{(n+1)} - \frac{1}{i\hbar}[qx, \rho^{(n)}]_{ij}E(t)\right]. \tag{25}$$

As the density matrix ρ has been obtained, the electronic polarization $P(t)$ and susceptibility $\chi(t)$ can be calculated as:

$$P(t) = \varepsilon_o\chi(\omega)Ee^{-i\omega t} + \varepsilon_o\chi(-\omega)Ee^{-i\omega t} = \frac{1}{V}\,\mathrm{Tr}(\rho M), \tag{26}$$

where ρ is the density matrix for one electron and V is the volume of the system, ε_0 represents permittivity of free space, and the symbol Tr (trace) denotes the summation over the diagonal elements of the matrix.

Now, using the real part of the susceptibility, refractive index changes can be determined as:

$$\frac{\Delta n(\omega)}{n_r} = \mathrm{Re}\left[\frac{\chi(\omega)}{2n_r^2}\right]. \tag{27}$$

Within a two-level system approach, the linear and the third order nonlinear optical absorption coefficient are obtained from the imaginary part of the susceptibility [25, 34, 45–51] as:

$$\alpha^{(1)}(\omega) = \omega\sqrt{\frac{\mu}{\varepsilon_r}}\frac{|M_{01}|^2 N\hbar\Gamma_0}{[(E_{10} - \hbar\omega)^2 + (\hbar\Gamma_0)]^2}, \tag{28}$$

$$\alpha^{(3,I)}(\omega) = -2\omega\sqrt{\frac{\mu}{\varepsilon_r}}\left(\frac{I}{\varepsilon_0\eta_r c}\right)\frac{|M_{01}|^4 N\hbar\Gamma_0}{\left[(E_{10} - \hbar\omega)^2 + (\hbar\Gamma_0)\right]^2} \times\left(1 - \frac{|M_{11} - M_{00}|^2}{4\,|M_{01}|^2}\left\{\frac{(E_{10} - \hbar\omega)^2 - (\hbar\Gamma_0)^2 + 2E_{10}(E_{10} - \hbar\omega)}{(E_{10})^2 + (\hbar\Gamma_0)^2}\right\}\right). \tag{29}$$

Total absorption coefficient $\alpha(\omega, I)$ is given as:

$$\alpha(\omega, I) = \alpha^{(1)}(\omega) + \alpha^{(3,I)}(\omega). \tag{30}$$

The linear and nonlinear changes in the refractive index are written as [25, 30, 46–54]:

$$\frac{\Delta\eta^{(1)}(\omega)}{\eta_r} = \frac{1}{2\eta_r^2\varepsilon_{\partial 0}}\,|M_{01}|^2\left[\frac{E_{10} - \hbar\omega}{(E_{10} - \hbar\omega)^2 + (\hbar\Gamma_0)^2}\right], \tag{31}$$

$$\frac{\Delta\eta^{(3,I)}(\omega,I)}{\eta_r} = -\frac{\mu c}{4\eta_r^3\varepsilon_{\partial 0}}\left|M_{01}\right|^2\left[\frac{NI}{[(E_{10}-\hbar\omega)^2+(\hbar\Gamma_0)^2]^2}\right] \times\left[4(E_{10}-\hbar\omega)\left|M_{01}\right|^2-\frac{\left|M_{11}-M_{00}\right|^2}{(E_{10})^2+(\hbar\Gamma_0)^2}\left\{E_{10}(E_{10}-\hbar\omega)\times-(\hbar\Gamma_0)^2(2E_{10}-\hbar\omega)\right\}\right]. \quad (32)$$

The total refractive index change is

$$\frac{\Delta\eta(\omega,I)}{\eta_r} = \frac{\Delta\eta^{(1)}(\omega)}{\eta_r} + \frac{\Delta\eta^{(3,I)}(\omega,I)}{\eta_r}, \quad (33)$$

where $\mu_{ij} = |\langle\psi_i|z_{T1}|\psi_j\rangle|$, $(i,j=0,1)$ are the matrix elements of the dipole moment, $\psi_i(\psi_j)$ are the eigenfunctions, $\omega_{01} = \dfrac{E_1-E_0}{\hbar}$ is the difference between two energy levels, is the frequency of the electromagnetic field, τ_0 is the relaxation time.

3. Results and discussions

We have considered the GaAs semiconductor material constants for our numerical results. We used the numerical parameters such as [38, 40–44] $m_e^* = 0.067m_0$, $m_h^* = 0.09m_0$ (m_0 is the mass of a free electron), $N = 3\cdot10^{22}$ m^{-3}, $\varepsilon = 12.53$, $\tau_0 = 0.2$ ps^{-1}, $I = 2000$ MW/m^2.

To understand the effect of change in hydrostatic pressure and temperature on the Linear Absorption Coefficient (LAC) and third order (Nonlinear) Absorption coefficient (NAC), we present the same in Fig. 2(a) and 2(b). Here we also have shown the effects of inclusion of Excitonic Effects (EE) on the LAC and NAC. One can observe that for the cases where (2(a) and 2(b)) the EE is not included, the NAC and LAC peaks occurred at photon energies much lower than the cases of inclusion of EE in the study. This is attributed to the energy associated with the excitonic interactions between the electron and holes. Moreover, the peak heights, for both LAC and Total Absorption Coefficient (TAC), increased when excitonic effects are taken into account. This is a consequence of enhancement of the dipole moment due to the positive-negative charge separation of the electron-hole pair, which otherwise is not there in the case of Without Excitonic Effects (WEE). In Fig. 2(a), shift from 60.28 to 56.70 meV when pressure is increased from 10 to 100 kbar in case of WEE. Whereas for identical change in pressure, the LAC and NAC peaks are shifted from 91.78 to 88.58 meV for the case of EE. This shifting is accompanied by decrease in absorption LAC peak height from $0.35\cdot10^5$ to $0.32\cdot10^5$ m^{-1} in case of WEE and from $0.80\cdot10^5$ to $0.72\cdot10^5$ m^{-1} for the EE case. Similar effects are also observed for the NAC. The LAC and NAC shift towards the lower energy end of the spectrum as the pressure increases. This shifting is accompanied by a diminishing absorption peak height for both EE and WEE case. These effects are due to the counter affecting action of pressure on the confinement potential and energy band gap. The pressure increases the confinement strength but it also strongly alters the energy band gap. For GaAs, in the pressure range of 10 kbar to 100 bar, these two opposing effects results in a net red shift of the peaks as the pressure increases. Whereas, in Fig. 2(b), one can see that the absorption peaks, LAC and NAC, moves from 60.28 to 62.40 meV and peak heights of LAC increase from $0.35\cdot10^5$ to $0.39\cdot10^5$ m^{-1} and NAC changes from $-0.062\cdot10^5$ to $-0.066\cdot10^5$ m^{-1} when the temperature increases from 10 to 100 K, keeping $P = 10$ kbar. For the case of EE, the blue shift in peaks happen from 91.7 to 94.39 meV and the LAC peak heights change from $0.80\cdot10^5$ to $0.85\cdot10^5$ m^{-1} and the NAC peak enhances from $-0.13\cdot10^5$ to $-0.17\cdot10^5$ m^{-1} as the temperature increases from 10 to 100 K. These effects, similar in nature for both EE and WEE, result from the interplay complex second term of Eq. (5) and the direct dependence of on the temperature. Physically, the change in the entropy of the charge carriers induces a change in the energy of the states. In Fig. 3(a,b), we present the TAC as a function of incoming photon energy. Here, we observe similar effects of change in pressure and temperature on the TAC peaks as in the case of LAC and NAC. However, in TAC, the effects of LAC dominate the NAC for the light intensity of 2000 MW/m^2. Furthermore, owing to the diametrically opposed behavior of the first and the third-order nonlinear ACs, a decrease in the total ACs is observed due to the reduction in the effective mass of the electron with the intensification of the temperature. A close relationship between the peak values of the total ACs, the transition dipole element and the difference between energy levels E_{10} can be disclosed from the figure. Total ACs is influenced in opposite by the dipole matrix element $|M_{10}|^2$ to that of the energy difference E_{10}. Hence, a blue shift is observed as a result of increase in the temperature and the red shift is observed when the pressure increases. This happens due to increase/decrease in the transition energy E_{10} on a significant increase in temperature/pressure. Upon increasing temperature/pressure, a drop/enhancement in the electron effective mass with an expansion/compression of the transition energy is observed due to the dependence of the electron-photon interaction of the temperature/pressure. Hence, the blue/red shift is observed. Same can be observed from Fig. 2(c,d) that how matrix elements get vary with pressure and temperature.

To compare our results in Fig. 3(b), we plotted the total absorption coefficient and compared with experimental data [55, 56] at $T \cong 10$ and 100 K. As it can be observed from the graph, a similar pattern is observed in both the experimental results as well as theoretical results but deviation can be observed in the theoretical prediction from the experimental data [55, 56]. At $T = 10$ K, the quantitative value is similar to the experimental value but this is not the same for the $T = 100$ K. Although, it can be observed from both experimental values as well as theoretical values that a

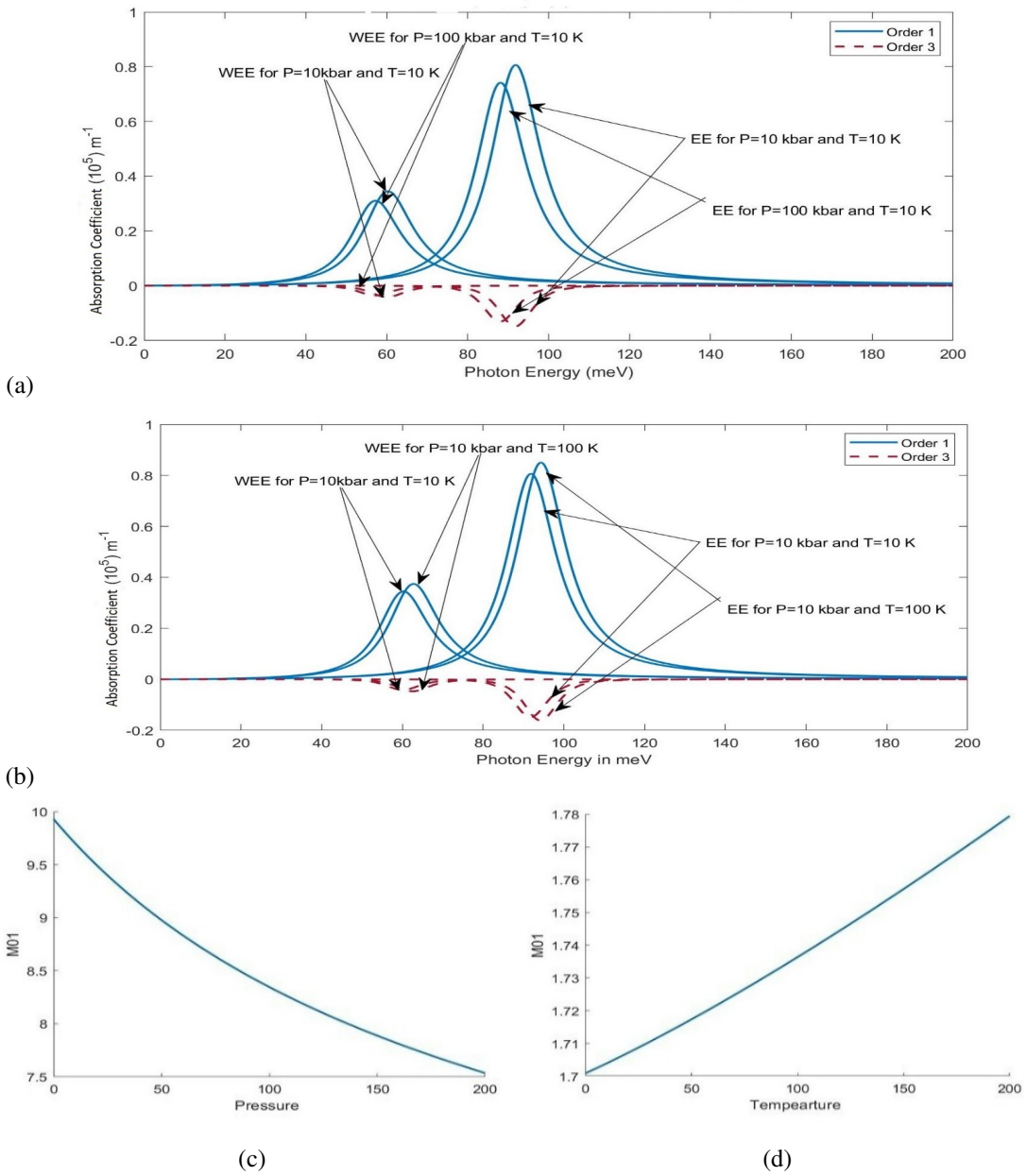

FIG. 2. (a,b) – the linear and nonlinear absorption coefficients with and without considering excitonic (EE and WEE) effects for $T = 10$ and 100 K and $P = 10$ kbar and $P = 100$ kbar and $I = 2000$ MWm^2; (c,d) – behavior of matrix element with pressure and temperature

blue shift is happening in the absorption coefficient on increasing the temperature. For example, for temperature between 0 – 20 and 40 – 100 K peaks shift towards higher energy values for the both cases, i.e., theoretical and experimental. But as there was no significant difference between the peaks ranging from 21 – 90 K, hence, only values for 20 and 100 K have been presented in the theoretical graphs. Several points can be thought of as a cause for this deviation in the quantitative value. Some of these points are: (i) electronic transitions are not perfectly exact for the two-level system, (ii) several parameters such as dot size, intensity, σ, υ are temperature dependent but are here considered as temperature independent, (iii) calculations have been performed theoretically using numerical methods and these methods have some limitations, (iv) approximation have been taken into account for solving the Eqs. (23–27).

As the interacting light changes the physical nature of the quantum dot material, it, therefore induces drastic changes in the refractive index of the QDs near the resonance energy. The same can be observed from the dispersion curves presented in Fig. 4(a,b) and 4(c,d). In 4(a), for WEE and hydrostatic pressure of 10 kbar, the dispersion curve of Linear Refractive Index change (LRI) rises to a maximum value 0.062 at photon energy 60.28 meV and crosses over to the negative polarity region to reach -0.063 at photon energy 74.40 meV. When the pressure increases to 100 kbar, this dispersion area shifts to 56.70 meV (maxima of 0.059) and 64.86 meV (minima of -0.059). Further, in 4(a), for pressure of 10 kbar, when EE is taken into account the area of polarity change of the LRI shifts to higher photon energy, viz. reaches

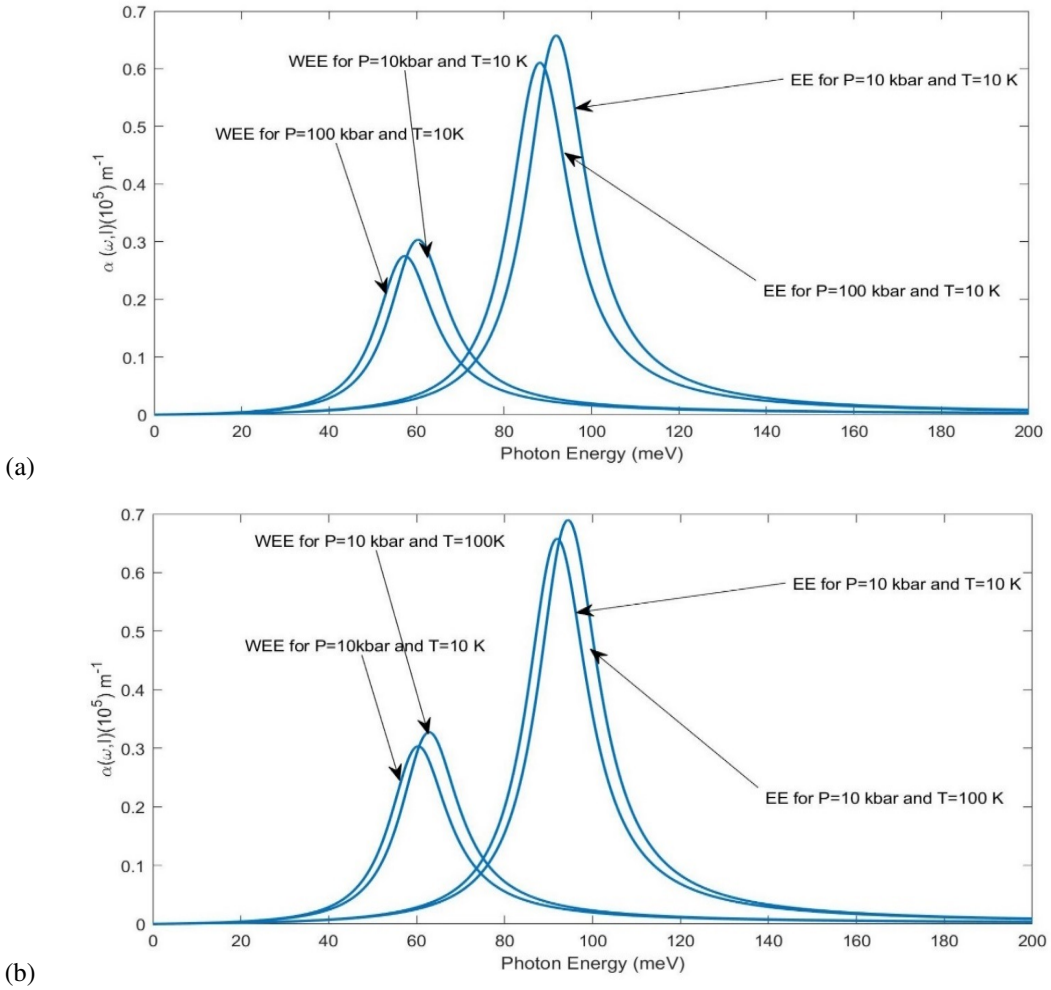

FIG. 3. Total absorption coefficients with and without considering excitonic (EE & WEE) effects for $T = 10$ & 100 K and $P = 10$ & $P = 100$ kbar and $I = 2000$ MWm^{-2}

maximum at photon energy 91.7 meV (maxima of 0.088) and crosses over to the negative values to reach the minimum value at 106.33 meV (minima of -0.088). Again, for EE case, when pressure increases to 100 kbar, the dispersion area red shifts to 88.58 meV (maxima 0.085) and 103.48 meV (minima -0.086). Similar effects are observed (Fig. 4(b)) for Nonlinear Refractive Index change (NRI) at the identical photon energies as in the case of LRI. However, in case of NRI, the polarity of the refractive index change first reaches a negative valued minima and then crosses over to a positive valued maximum. Opposite nature of shifting of the dispersion is observed when the temperature is changed from 10 to 100 K keeping $P = 10$ kbar (Fig. 4(c,d)). In Fig. 4(c), it is obtained that the maximum value of the LRI (minimum value of NRI in Fig. 4(d)) occurs at photon energy 60.28 meV (maxima of 0.062) when the temperature is kept at 10 K for the case of WEE. When the temperature increases to 100 K, in case of WEE, the maximum value of the LRI (minimum of NRI, Fig. 4(d)) shifts to a higher photon energy value of 62.40 meV. Whereas for the case of EE, the LRI (and NRI) maximum value (minima for NRI) shifts from 91.7 to 94.39 meV when the temperature increases to 100 from 10 K. These two-opposite natures of influences on the RI change of hydrostatic pressure and temperature are attributed to the fact that the increase in pressure strengthens the confinement whereas the temperature acts the other way.

In Fig. 5(a,b), the total refractive index change is presented at two values of applied hydrostatic pressure (5a) keeping $T = 10$ K and in (5b), the temperature is varied from 10 to 100 K keeping $P = 10$ kbar. It can be observed that the magnitude of the change in refractive index with variation in hydrostatic pressure and temperature are different on the two scenarios, i.e., one with the excitonic effect and the other without excitonic effects. This is the consequence of the fact that in case of WEE, the properties are determined by the effective mass of the electron whereas in case of EE, the properties are manifested from the reduced mass of the electron-hole pair. This is one of the major factors for variation in the optical properties in between EE and WEE, in addition to the fact of opposite polarity charges being involved in the case of EE.

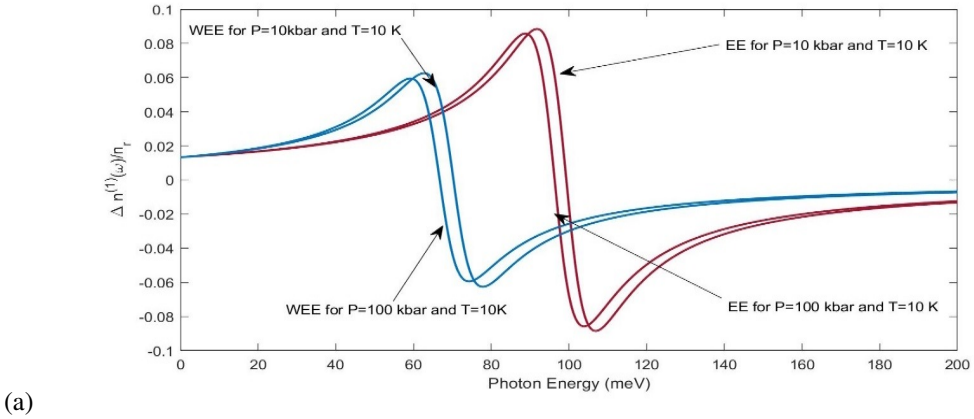

(a)

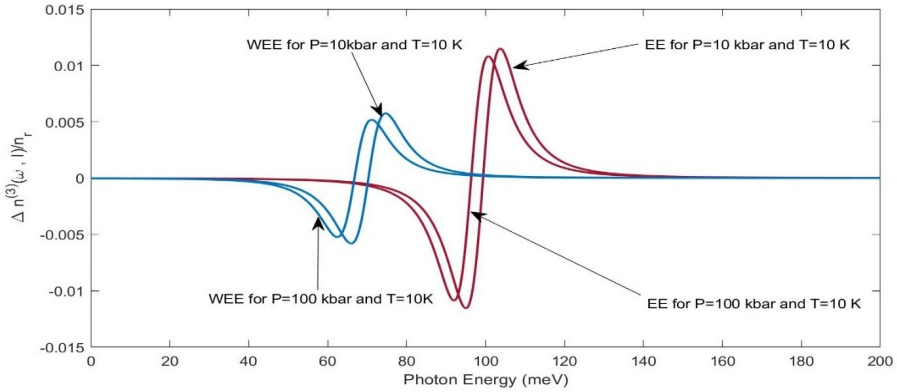

(b)

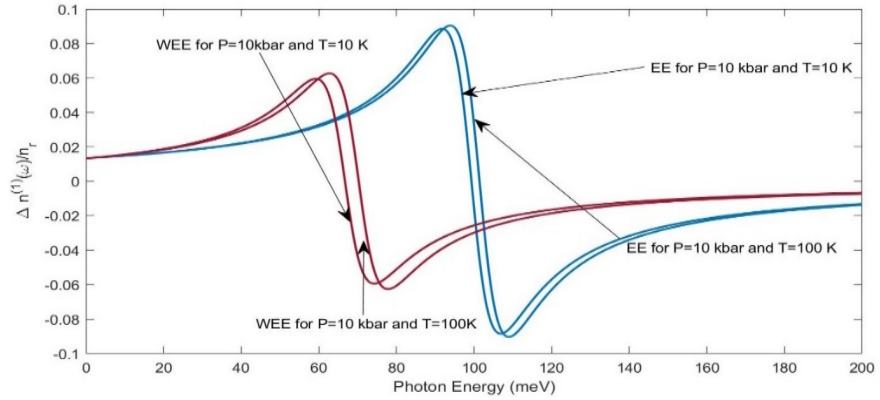

(c)

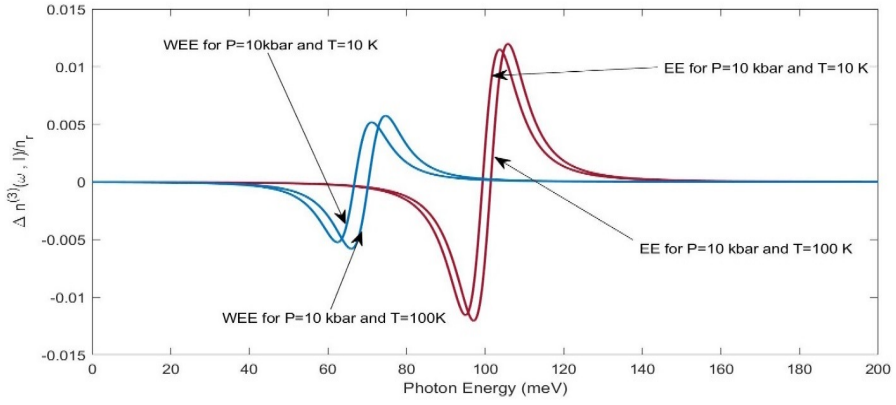

(d)

FIG. 4. Schematic diagram of GaAs Quantum Dot.The linear and nonlinear refractive index for with and without considering excitonic (EE & WEE) effects for $T = 10$ and 100 K and $P = 10$ kbar and $P = 100$ kbar and $I = 2000$ MWm^{-2}

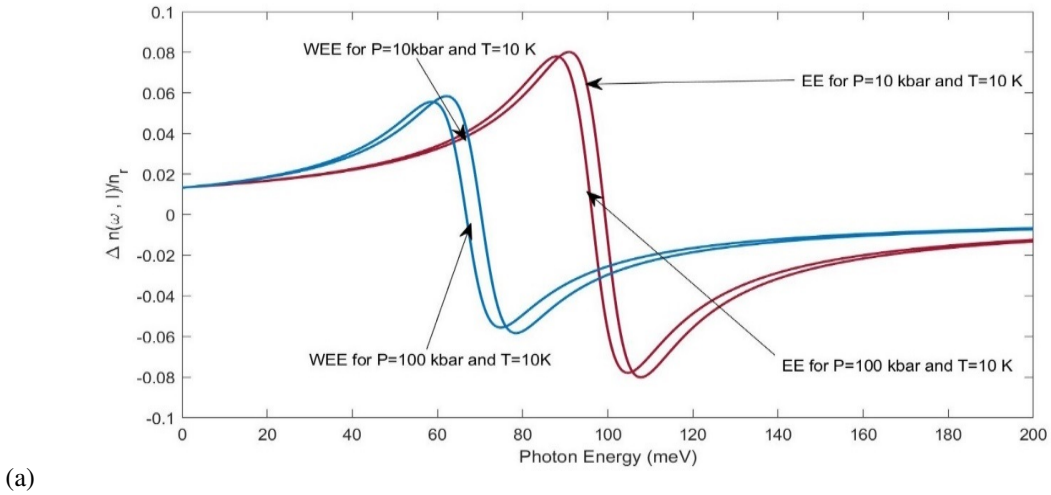

(a)

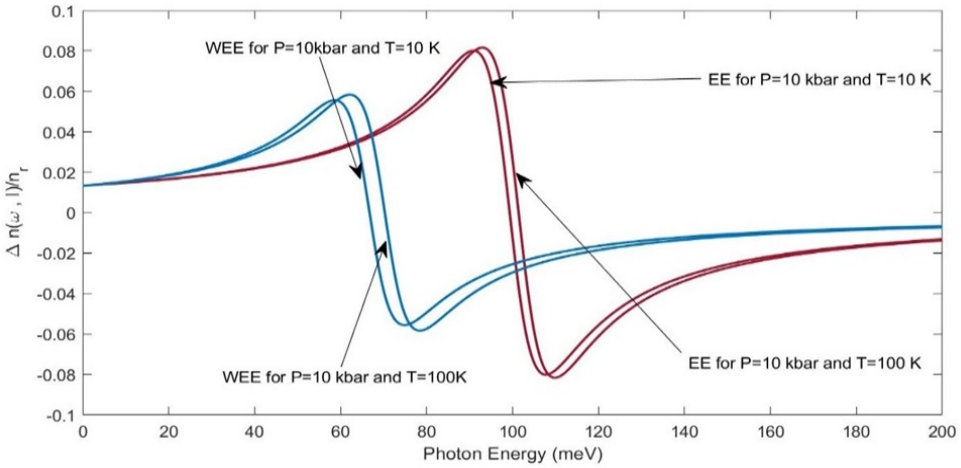

(b)

FIG. 5. The total refractive index for with and without considering excitonic (EE and WEE) effects for $T = 10$ and 100 K and $P = 10$ kbar and $P = 100$ kbar and $I = 2000$ MWm^{-2}

4. Conclusion

We have reported the linear and nonlinear optical properties, viz. absorption coefficient and refractive index of a GaAs semi-parabolic QD by employing the compact density matrix formalism. We have demonstrated that the absorption coefficient peaks and refractive index dispersion variation is blue shifted with the inclusion of excitonic effects. The increase in the pressure alters the optical properties of the QD by controlling the effective mass of electron, energy band gap and the dielectric constant. This intricate counter-balancing act results in a red shift in the nonlinear optical properties' resonance position when the applied hydrostatic pressure is incremented, while augmenting the ambient temperature results in blue shifts of the LAC, NAC and TAC and refractive index change. Further, it is observed that the enhancing the pressure lowers the peak height of the absorption coefficient and the refractive index dispersions curves. This is due to the diminishing of dipole moments of the QD by the reinforcing the confinement by the hydrostatic pressure which results in shrinking of the orbital wave functions. To our best knowledge no such research work illustrating the effects of Hydrostatic Pressure and Temperature on the RI and AC (Linear and third order) of GaAs QD for a semi-parabolic system (excitonic as well as non-excitonic cases) has been carried out earlier. According to our consideration, the obtained results can have important practical applications in fabricating optoelectronic devices and hence have a sound share in progressive product technology. The shifting of absorption peaks can specially be used in devices where optical switches can be turned on and off depending on absorption of incident radiation. Hydrostatic pressure and temperature can act as external parameters. Further, the same property may also be used to detect changes in temperature and pressure by observing the refractive index change and absorption of photons at particular wavelength. Analysis of the experimental results [55, 56] and comparing with the theoretical results obtained, some disagreement is observed in the absorption coefficients. This variation with the experimental results is explained in the previous section.

References

[1] Jamieson T., Bakhshi R., Petrova D., Pocock R., Imani M., Seifalian A.M. Biological applications of quantum dots. *Biomaterials*, 2007, **28** (31), P. 4717–4732.

[2] Salata O. Applications of nanoparticles in biology and medicine. *J. Nanobiotechnol.*, 2004 **2** (1), 3.

[3] Mocatta D., Cohen G., Schattner J., Millo O., Rabani E., Banin U. Heavily doped semiconductor nanocrystal quantum dots. *Science*, 2011, **332** (6025), P. 77–81.

[4] Koenraad P.M, Flatté M.E. Single dopants in semiconductors. *Nat. Mater.*, 2011, **10**, P. 91–100.

[5] Aghoutane N., Pérez L.M., Tiutiunnyk A., Laroze D., Baskoutas S., Dujardin F., Fatimy A.E., El-Yadri M., Feddi E.M. Adjustment of Terahertz Properties Assigned to the First Lowest Transition of (D+, X) Excitonic Complex in a Single Spherical Quantum Dot Using Temperature and Pressure. *Applied Sciences*, 2021, **11** (13), 5969.

[6] Schneider H., Fuchs F., Dischler B., Ralston J.D., Koidl P. Intersubband absorption and infrared photodetection at 3.5 and 4.2 μm in GaAs quantum wells. *Appl. Phys. Lett.*, 1991, **58**, P. 2234–2236.

[7] Ferry D.K., Goodnick S.M. *Transport in Nanostructures*. Cambridge University Press, Cambridge, 1997.

[8] Sarkisyan H.A. Direct optical absorption in cylindrical quantum dot. *Mod. Phys. Lett. B*, 2004, **18** (10), P. 443–452.

[9] Saravanamoorthy S.N., John Peter A., Lee C.W. Optical peak gain in a PbSe/CdSe core-shell quantum dot in the presence of magnetic field for mid-infrared laser applications. *Chem. Phys.*, 2017, **483–484**, P. 1–6.

[10] Bera A., Ghosh M. Dipole moment and polarizability of impurity doped quantum dots driven by noise: Influence of hydrostatic pressure and temperature. *Physica B*, 2017, **515**, P. 18–22.

[11] Schaller R.D., Klimov V.I. High Efficiency Carrier Multiplication in PbSe Nanocrystals: Implications for Solar Energy Conversion. *Phys. Rev. Lett.*, 2004, **92** (18), 186601.

[12] Huynh W.U., Dittmer J.J., Alivisatos A.P. Hybrid nanorod-polymer solar cells. *Science*, 2002, **295** (5564), P. 2425–2427.

[13] Zhong X., Xie R., Basche Y., Zhang T., Knoll W. High-Quality Violet- to Red-Emitting ZnSe/CdSe Core/Shell Nanocrystals. *Chem. Mater., Chem. Mater.*, 2005, **17** (16), P. 4038–4042.

[14] Ungan F., Mart´ınez-Orozco J.C., Restrepo R.L., Mora-Ramos M.E., Kasapoglu E., Duque C.A. Nonlinear optical rectification and second-harmonic generation in a semi-parabolic quantum well under intense laser field: Effects of electric and magnetic fields. *Superlattice Microstruct.*, 2015, **81**, 26.

[15] Karimi M.J., Rezaei G. Effects of external electric and magnetic fields on the linear and nonlinear intersubband optical properties of finite semi-parabolic quantum dots. *Physica B*, 2011, **406**, 4423.

[16] Fl´orez J., Camacho A. Excitonic effects on the second-order nonlinear optical properties of semi-spherical quantum dots. *Nanoscale Res. Lett.*, 2011, **6**, 268.

[17] Cristea M. Comparative study of the exciton states in CdSe/ZnS core-shell quantum dots under applied electric fields with and without permanent electric dipole moment. *Eur. Phys. J. Plus*, 2016, **131**, 86.

[18] Chaurasiya R., Dahiya S., Sharma R. A study of confined Stark effect, hydrostatic pressure and temperature on nonlinear optical properties in 1D GaxAl1-xAs/GaAs/GaxAl1-xAs quantum dots under a finite square well potential. *Nanosystems: Phys. Chem. Math.*, 2023, **14** (1), P. 44–53.

[19] Eseanu N. Simultaneous effects of laser field and hydrostatic pressure on the intersubband transitions in square and parabolic quantum wells. *Phys. Lett. A*, 2010, **374**, 1278.

[20] Rezaei G., Karimi M.J., Keshavarz A. Excitonic effects on the nonlinear intersubband optical properties of a semi-parabolic one-dimensional quantum dot. *Physica E*, 2010, **43**, 475.

[21] Yuan H.J., Zhang Y., Mo H., Chen N., Zhang Z.-H. Electric field effect on the second-order nonlinear optical properties in semiparabolic quantum wells. *Physica E*, 2016, **77**, 102.

[22] Karabulut I., Safak H., Tomak M. Nonlinear optical rectification in asymmetrical semiparabolic quantum wells. *Solid State Commun.*, 2005, **135**, 735.

[23] Bautista J.E., Lyra M.L., Lima R.P.A. Screening effect on the exciton mediated nonlinear optical susceptibility of semiconductor quantum dots. *Photon. Nanostruct.*, 2013, **11**, 8.

[24] Paspalakis E., Boviatsis J., Baskoutas S. Effects of probe field intensity in nonlinear optical processes in asymmetric semiconductor quantum dots. *J. Appl. Phys.*, 2013, **114**, 153107.

[25] Karabulut I., Safak H., Tomak M. Excitonic effects on the nonlinear optical properties of small quantum dots. *J. Phys. D: Appl. Phys.*, 2008, **41**, 155104.

[26] Baghramyan H.M., Barseghyan M.G., Kirakosyan A.A., Restrepo R.L., Duque C.A. Linear and nonlinear optical absorption coefficients in GaAs/$Ga_{1-x}Al_x$As concentric double quantum rings: Effects of hydrostatic pressure and aluminum concentration. *J. Lumin.*, 2013, **134**, P. 594–599.

[27] Gambhir M., Varsha, Prasad V. Pressure- and temperature-dependent EIT studies in a parabolic quantum dot coupled with excitonic effects in a static magnetic field. *Pramana – J. Phys.*, 2022, **96**, 81.

[28] Gambhir M., Kumar P., Kumar T. Investigation of linear and third-order nonlinear optical properties in a laser-dressed parabolic quantum dot with a hydrogenic donor impurity in the presence of a static electric field. *Indian J. Phys.*, 2023, **97**, P. 2169–2178.

[29] Zhang L., Li X., Zhao Z. The influence of optical absorption under the external electric field and magnetic field of parabolic quantum dots. *Indian J. Phys.*, 2022, **96**, P. 3645–3650.

[30] Duan Y., Li X., Chang C. Effects of Magnetic Field on Nonlinear Optical Absorption in Quantum Dots Under Parabolic-Inverse Squared Plus Modified Gaussian Potential. *Braz. J. Phys.*, 2022, **52**, 123.

[31] Yu Y.-B., Zhu S.-N., Guo K.-X. Exciton effects on the nonlinear optical rectification in one-dimensional quantum dots. *Phys. Lett. A*, 2005, **175**, 335.

[32] Karabulut İ., Şafak H. Nonlinear optical rectification in semiparabolic quantum wells with an applied electric field. *Physica B*, 2005, **82**, 368.

[33] Duque C.M., Mora-Ramos M.E., Duque C.A. Simultaneous effects of electron-hole correlation, hydrostatic pressure, and temperature on the third harmonic generation in parabolic GaAs quantum dots. *J. Nanopart. Res.*, 2013, **13**, P. 6103–6112.

[34] Baskoutas S., Paspalakis E., Terzis A.F. Effects of excitons in nonlinear optical rectification in semiparabolic quantum dots. *Phys. Rev. B*, 2006, **74**, 153306.

[35] Duque C.A., Porras-Montenegro N., Barticevic Z., Pacheco M., Oliveira L.E. Effects of applied magnetic fields and hydrostatic pressure on the optical transitions in self-assembled InAs/GaAs quantum dots. *J. Phys.: Condens. Matter*, 2006, **18**, P. 1877–1884.

[36] Duque C.M., Morales A.L., Mora-Ramos M.E., Duque C.A. Optical nonlinearities associated to applied electric fields in parabolic two-dimensional quantum rings. *J. of Luminescence*, 2013, **143**, P. 81–88.

[37] Mughnetsyan V.N., Manaselyan Kh.A., Barseghyan M.G., Kirakosyan A.A. Simultaneous effects of hydrostatic pressure and spin-orbit coupling on linear and nonlinear intraband optical absorption coefficients in a GaAs quantum ring. *J. Lumin.*, 2013, **134**, P. 24–27.
[38] Duque C.M., Mora-Ramos M.E., Duque C.A. Hydrostatic pressure and electric field effects and nonlinear optical rectification of confined excitons in spherical quantum dots. *Superlattices and Microstructures*, 2011, **49**, P. 264–268.
[39] Bejan D. Exciton effects on the nonlinear optical properties of semiparabolic quantum dot under electric field. *Eur. Phys. J. Plus*, 2017, **132**, 102.
[40] Antil S., Kumar M., Lahon S., Dahiya S., Ohlan A., Punia R., Maan A.S. Influence of hydrostatic pressure and spin orbit interaction on optical properties in quantum wire. *Physica B: Condensed Matter*, 2019, **552**, P. 202–208.
[41] Antil S., Kumar M., Lahon S., Maan A.S. Pressure dependent optical properties of quantum dot with spin orbit interaction and magnetic field. *Optik – Int. J. for Light and Electron Optics*, 2019, **176**, P. 278–286.
[42] Dahiya S., Lahon S., Sharma R. Effects of temperature and hydrostatic pressure on the optical rectification associated with the excitonic system in a semi-parabolic quantum dot. *Physica E*, 2020, **118**, 113918.
[43] Braggio A., Grifoni M., Sassetti M., Napoli F. Plasmon and charge quantization effects in a double-barrier quantum wire. *Europhys. Lett.*, 2000, **50**, 236.
[44] Unlu S., Karabulut I., Safak H. Linear and nonlinear intersubband optical absorption coefficients and refractive index changes in a quantum box with finite confining potential. *Physica E*, 2006, **33**, 319.
[45] Fickenscher M., Shi T., Jackson Howard E., Smith Leigh M., Yarrison-Rice Jan M., Zheng C., Miller P., Etheridge J., Wong Bryan M., Gao Q., Deshpande S., Hoe Tan H., Jagadish C. Optical, Structural, and Numerical Investigations of GaAs/AlGaAs Core-Multishell Nanowire Quantum Well Tubes. *Nano Letters*, 2013, **13** (3), P. 1016–1022.
[46] Raigoza N., Morales A., Montes A., Porras-Montenegro N., C.A. Duque, Optical nonlinearities associated to applied electric fields in parabolic two-dimensional quantum rings. *Phys. Rev. B*, 2004, **69**, 045323.
[47] Oyoko H., Parras-Montenegro N., Lopez S., Duque C.A. Comparative study of the hydrostatic pressure and temperature effects on the impurity-related optical properties in single and double GaAs–$Ga_{1-x}Al_xAs$ quantum wells. *Phys. Status Solidi C*, 2007, **4**, 298.
[48] Herbert Li E. Material parameters of InGaAsP and InAlGaAs systems for use in quantum well structures at low and room temperatures. *Physica E*, 2000, **5**, 215.
[49] Haldane F.D.M. 'Luttinger liquid theory' of one-dimensional quantum fluids. I. Properties of the Luttinger model and their extension to the general 1D interacting spinless Fermi gas. *J. Phys. C*, 1981, **14**, 2585.
[50] Boyd R.W. *Nonlinear Optics*, Elsevier Science, 2020.
[51] Naghmaish Aishah AL., Dakhlaoui H., Ghrib T. Effects of magnetic, electric, and intense laser fields on the optical properties of AlGaAs/GaAs quantum wells for terahertz photodetectors. *Physica B: Condensed Matter*, 2022, **635**, 413838.
[52] Dahiya S., Lahon S., Sharma R. Study of third harmonic generation in $In_xGa_{1-x}As$ semi-parabolic 2-D quantum dot under the influence of Rashba spin-orbit interactions (SOI): Role of magnetic field, confining potential, temperature & hydrostatic pressure. *Physica E: Low-dimensional Systems and Nanostructures*, 2023, **147**, 115620.
[53] Kuhn K.J., Lyengar G.U., Yee S. Free carrier induced changes in the absorption and refractive index for interurban optical transitions in $Al_xGa_{1-x}As$/GaAs/$Al_xGa_{1-x}As$ quantum wells. *J. Appl. Phys.*, 1991, **70**, 5010.
[54] Kopf R.F., Herman M.H., Lamont Schnoes M., Perley A.P., Livescu G., Ohring M. Band offset determination in analog graded parabolic and triangular quantum wells of GaAs/AlGaAs and GaInAs/AlInAs. *J. Appl. Phys.*, 1992, **71** (10), P. 5004–5011.
[55] Gurmessa A., Melese G., Choudary V.L., Shewamare S. Photoluminescence from GaAs nanostructures. *Int. J. of Physical Sciences*, 2015, **10** (3), P. 106–111.
[56] Lourenc S.A., Dias I.F.L., Duart J.L., Laureto E., Aquino V.M., Harmand J.C. Temperature-Dependent Photoluminescence Spectra of GaAsSb/AlGaAs and GaAsSbN/GaAs Single Quantum Wells under Different Excitation Intensities. *Brazilian J. of Physics*, 2007, **37** (4), P. 1212–1217.

Submitted 29 July 2024; revised 26 August 2024; accepted 1 September 2024

Information about the authors:

Suman Dahiya – Department of Applied Physics, Delhi Technological University, Delhi 110042, India; ORCID 0000-0003-4815-5354

Siddhartha Lahon – Physics Department, KMC, University of Delhi, Delhi 110007, India; sid.lahon@gmail.com

Rinku Sharma – Department of Applied Physics, Delhi Technological University, Delhi 110042, India; ORCID 0000-0003-6812-4358; rinkusharma@dtu.ac.in

Conflict of interest: the authors declare no conflict of interest.